

High Contrast Imaging Upgrades for the Keck Adaptive Optics Imager

Sam Ragland¹, Dimitri Mawet^{2,3}, Carlos Alvarez¹, Keith Matthews², Charlotte Z. Bond¹, Sylvain Cetre¹, Jacques-Robert Delorme^{2,1}, Scott Lilley¹, Nemanja Jovanovic², Garreth Ruane³, Olivier Absil⁴, Mark Chun⁵, Daniel Echeverri², Sean Goebel⁵, Olivier Guyon⁶, Mikael Karlsson⁷, Charles Lockhart⁵, Maxwell Millar-Blanchaer³, Mojtaba Taheri⁸, J. Kent Wallace³, Eric Warmbier⁵, Ed Wetherell¹, Peter Wizinowich¹

¹W. M. Keck Observatory, Kamuela, Hawaii, USA. ²California Institute of Technology, CA, USA., ³Jet Propulsion Laboratory, CA, USA. ⁴University of Liege, Belgium. ⁵University of Hawaii, HI, USA. ⁶Subaru Telescope, HI, USA. ⁷Uppsala University, Sweden. ⁸University of Victoria, Canada

Email: sragland@keck.hawaii.edu

ABSTRACT

The Keck II adaptive optics (AO) system is being upgraded with a near-infrared Pyramid Wavefront Sensor (PWS) as part of the Keck Planet Imager and Characterizer (KPIC) upgrade. The overview of the KPIC project and the PWS development are presented elsewhere in this conference. This paper focuses on improvements made to the NIRC2 science instrument, referred to as the NIRC2 upgrade, aimed at enhancing its high contrast imaging capabilities. The NIRC2 upgrade incorporates new coronagraphic elements that reach their maximum performance when operated in combination with the new near-infrared PWS and polarimetric elements that would add polarimetric capability when fully implemented.

The key elements to the NIRC2 upgrade are the installation of two next-generation Vector Vortex Coronagraphic (VVC) masks, one optimized for the L and M band, and the other one optimized for the K band. Also key to the upgrade is the incorporation of a new Lyot stop optimized to minimize diffraction and residual nutation of the Keck-II telescope pupil. These new elements provide improved coronagraphic performance when operated with the new PWS and the existing Shack Hartmann wavefront sensor (SH WFS). The upgrade implementation and preliminary on-sky results are discussed.

Keywords: Keck Planet Imager and Characterizer, Pyramid wavefront sensor, high-contrast imaging, coronagraph, vortex phase mask

1. INTRODUCTION

We are in the process of upgrading NIRC2, which is the workhorse AO-fed infrared science imager and spectrograph at the Keck II telescope. The goals of the upgrade are to mitigate obsolescence while enhancing the efficiency of NIRC2 for all of its science users, to optimize the thermal infrared small-angle exoplanet imaging capabilities, to extend coronagraphy to longer wavelengths (M band), and to provide a new differential polarimetry mode for the study of exoplanets and protoplanetary, transitional and debris circumstellar disks.

NIRC2 was upgraded in 2015 with two first-generation L-band (3.7 μ m) vortex coronagraphic masks based on an Annular Groove Phase Mask made up of a diamond sub-wavelength grating. The vortex coronagraphic observations in the L-band benefit from the favorable star/planet contrast ratio and the relatively high Strehl ratio at the longer wavelengths. The vortex coronagraphic mode produced interesting technical and scientific results (Serabyn et al., 2017; Mawet et al., 2017; Huby et al., 2017; Ruane et al., 2017; Reggiani et al., 2018), and provided the Keck community with a facility instrument able to match the sensitivity of second-generation extreme adaptive optics systems.

NIRC2 was upgraded again in February-March 2019 to maximize its performance and capabilities for high contrast imaging. The NIRC2 upgrade, funded by contributions from Jeff and Rebecca Steele, extends the coronagraphic capabilities of NIRC2 to the K and the M band, enabling new science in the area of exoplanet and circumstellar disk studies. The upgrade includes the implementation of (1) two next-generation Vector Vortex Coronagraphic (VVC) masks - one optimized for the L and M bands and the other one optimized for the K band, (2) a new mask holder to ensure that the masks are placed close to the detector center, enabling fast readout using sub-array windowing, and (3) a new Lyot stop optimized for the Keck II telescope hexagonal pupil to maximize throughput while minimizing diffracted starlight

and the thermal emission from the secondary mirror spiders. The upgrade also includes the implementation of a Wollaston prism and a field mask for the polarimetric mode. The status of the upgrade in conjunction with the development of the infrared Pyramid Wavefront Sensor (PWS) for Keck II is presented along with some initial results.

The outline of the paper is as follows: The overview of the upgrade is briefly described in Section 2, the details on coronagraphic and polarimetric modes are presented in Sections 3 & 4 respectively, the details on the observing sequencer and on-axis performance are presented in Sections 5, and a brief summary and the future plans in Section 6.

2. OVERVIEW

The upgrade includes new opto-mechanical components in the NIRC2 dewar, modifications to the operation software and daytime calibration procedures, and upgrades to the observing sequencer for high contrast imaging coronagraphy with the vortex masks.

Figure 1 illustrates the main opto-mechanical components in the NIRC2 dewar. The light from the telescope is propagated through the AO system and enters the dewar at the CaF₂ entrance window. Once in the dewar, the light passes through the outer and inner pre-slit linear stages. These linear stages contain different baffling options depending on which camera is selected. Next in the optical path are the slit and the mask linear stages. The slit linear stage contains a variety of coronagraphic spots and long slits for spectroscopy. The mask linear stage contains several baffling options depending on the observing mode. The diverging beam emerging from the focal plane is sent to the collimator, followed by the pupil wheel and the two filter wheels. The pupil wheel can host up to six masks, four of which are connected to a pupil mask rotation mechanism. The collimated beam continues to the grism exchanging stage through a mechanically actuated shutter. The shutter is just behind the Inner Filter Wheel (FWI) and the Grism Stage (GS). The GS contains a medium resolution grism, a low-resolution grism, and a pupil imaging lens. Finally, the light is sent to the detector through one of the three available cameras (10, 20 and 40 mas/pix).

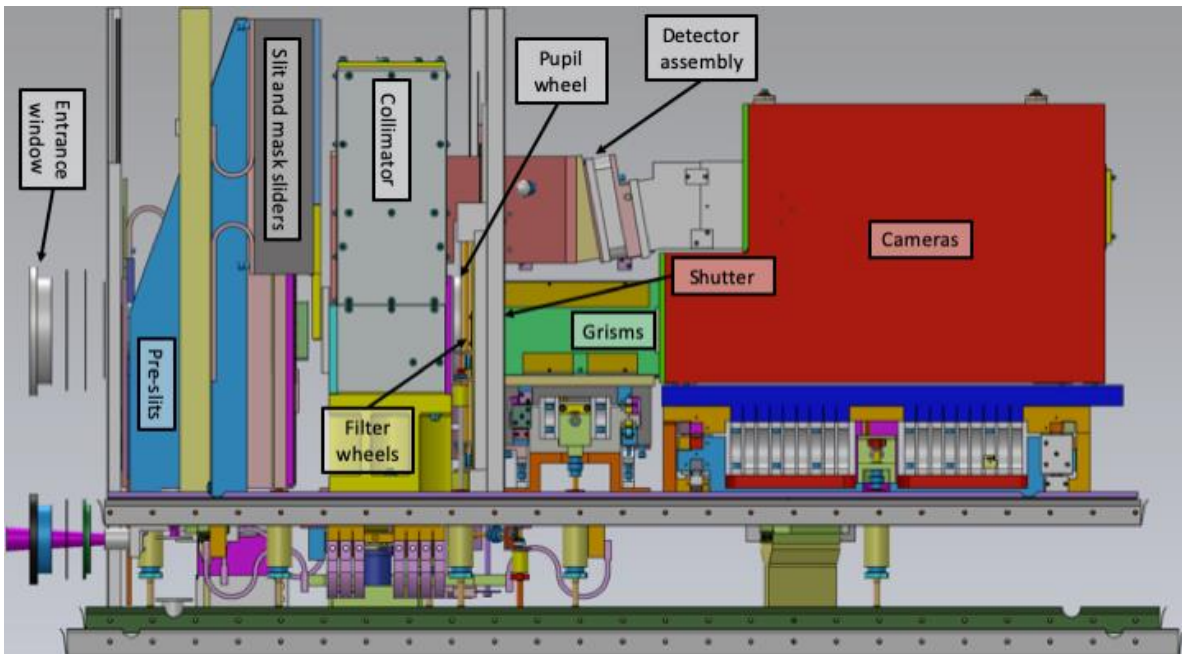


Figure 1: Solidworks model showing the main opto-mechanical components of the NIRC2 dewar (see text for description.)

A schematic diagram of the NIRC2 dewar with the opto-mechanical elements included in the current upgrade and planned for the future is shown in Figure 2. The polarimetry field masks and the vortex masks were installed on the mask and slit linear stages, respectively. The new Lyot stop replaced a little-used special purposes Lyot stop and is not suitable for observations in position angle mode, i.e. with the sky fixed on the detector plane. The Wollaston prism was mounted on the outer filter wheel. The Wollaston replaced a position on the wheel previously occupied by a blank block. Therefore, no filter needed to be removed to add the new polarimetric capability.

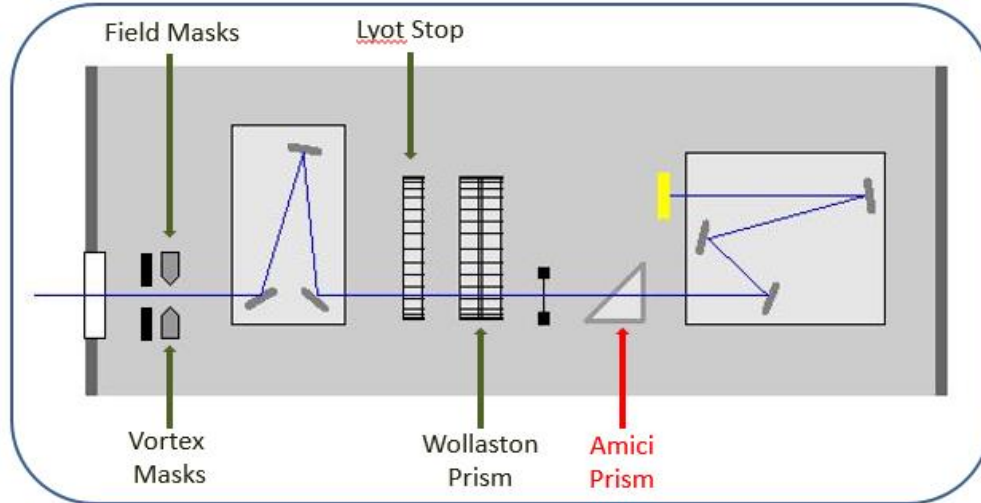


Figure 2: Schematic diagram of the NIRC2 dewar with new optics marked with green arrows. The Amici Prism marked with a red arrow is yet to be installed as part of a future spectro-polarimetric mode.

The core of the upgrade took place between February 17th and March 19th, 2019. The work included a one-week long dewar warm-up phase, one day to open the dewar (see Figure 3), three days to install the new optomechanical components and to close the dewar, two additional days to perform preventative maintenance tasks, including the replacement of the dewar cold heads, one week to cool down the dewar, a period of daytime testing and two half nights of on-sky commissioning. Additional daytime testing and on-sky commissioning outside this period were needed to optimize the operation software and observing procedures.

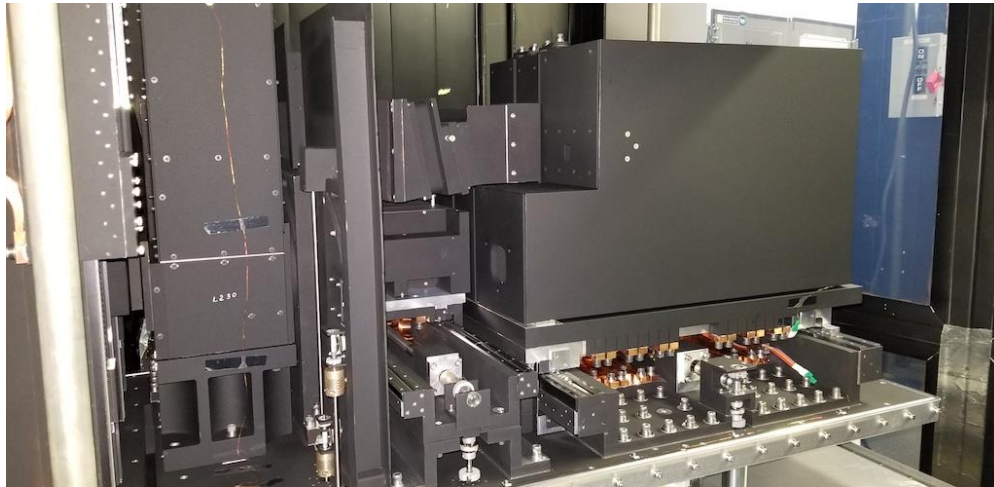


Figure 3: NIRC2 dewar minutes after being opened on February 25th, 2019.

3. CORONAGRAPHY

The earlier NIRC2 upgrade involved the installation of two L-band vortex coronagraphic masks. The current upgrade includes two new vortex masks - one optimized for the L- and M-bands and the other one for the K-band. The masks were manufactured using lithographic process: resist e-beam writing and reactive ion etching of a synthetic diamond substrate. The mask holder has been remanufactured to position both coronagraphic masks closer to the detector center enabling short exposure sub-frame readout. The new Lyot stop was implemented to (1) reduce stellar leakage by masking the spiders, (2) improve throughput for the companion by not blocking more of the pupil than is needed, (3) reduce background from the spiders upstream, and (4) reduce residual pupil nutation. A photograph of the vortex mask and the pupil stop are shown in Figure 4.

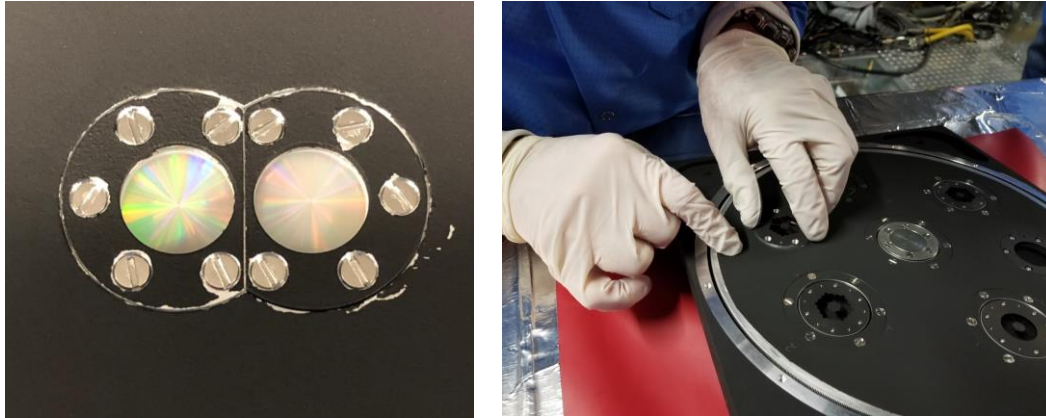


Figure 4: Left: A photograph of the two new Vortex coronagraphic masks installed on the slit stage. Right: Keith Matthews installing the new pupil stop optimized for coronagraphy.

The new vortex masks were named *vortexk* and *vortexlm* on the NIRC2 control software, for the K-band and L/M-band optimized masks, respectively. They are inserted in the optical path using the command `vcorona <maskname>` on a NIRC2 control terminal. The approximate location of the masks is pixel [548, 525] and pixel [541,498] on the 1024x1024 InSb Aladdin-III array for the K-band and L/M-band vortex masks, respectively. This central location of the masks enables the utilization of detector sub-windows for fast readout. The efficiency of the observations in the thermal infrared regime has improved by nearly a factor of two with respect to the observations using the previous version of the vortex mask.

The new Lyot stop follows the shape of the Keck-II telescope pupil, including slightly oversized bars to block the secondary mirror spider and the central obscuration. The stop is referred to as *fixedhex* on the NIRC2 control system and it can be inserted in the optical path with the command `pupil fixedhex`. This is a non-rotating mask. Therefore, the AO de-rotator should be used to match the telescope pupil to the mask when observing in vertical angle mode. The rotator angle that ensures the pupil-to-Lyot matching is 3.73 deg.

4. POLARIMETRY

The polarimetric upgrade to NIRC2 will allow for new exciting science at Keck in a range of fields, including exoplanet science. The upgrade involves the implementation of a Wollaston prism (an analyzer for imaging polarimetry) and a field mask inside the NIRC2 dewar, and a yet to be installed half-wave plate (a rotatable modulator) outside the dewar. A photograph of the Wollaston prism is shown in Figure 5. The Wollaston has over 90% transmission from 1 μ m to 4.5 μ m and it was manufactured by United Crystals Inc.



Figure 5: Keith Matthews holding the Wollaston prism.

The Wollaston prism was installed in position number 14 of the outer filter wheel. The command *filt* was modified to accept the named position *Wollaston*. Additionally, the command *impol <filter>* was added to the suite of NIRC2 operation scripts in order to insert in the optical path the Wollaston prism and a compatible filter. To observe in imaging polarimetry mode, it is also necessary to insert the 5'' wide mask in the optical path, which only lets light through a 5'' wide horizontal band at the first focal plane. At the detector, the image is 10'' wide, consisting of two 5'' wide orthogonally polarized images. The imaging polarimetry mask is referred to as *5arcsec_wide* in the NIRC2 control software and it is located in the mask linear stage. The mask linear stage also contains the *5arcsec_slot*, designed to be used in spectro-polarimetry mode.

5. ON-SKY PERFORMANCE

The Vortex observing sequencer, QACITs (Huby et al., 2016, Huby et al., 2017), was upgraded for coronagraphic observations using the newly commissioned near-infrared PWS and the newly installed vortex masks. The upgrade would enable improved performance for the standard Shack Hartmann wavefront sensor as well as the PWS.

The main changes to the observing sequencer are (1) the use of the PWS modulator to point and track the on-sky target simultaneously on the PWS and the vortex mask, (2) the use of the PWS modulator for differential pointing between the PWS and the vortex mask for off-axis PSF measurements, and (3) and the control of the PWS loops.

The upgraded coronagraph and the observing sequencer were tested on the sky using the PWS. Additionally, we have carried out several shared-risk science observations. A set of sample on-sky images in the L' filter are shown in Figure 6 for two cases: (1) when the target is off-centered with respect to the vortex mask, and (2) when the target is aligned to the vortex mask.

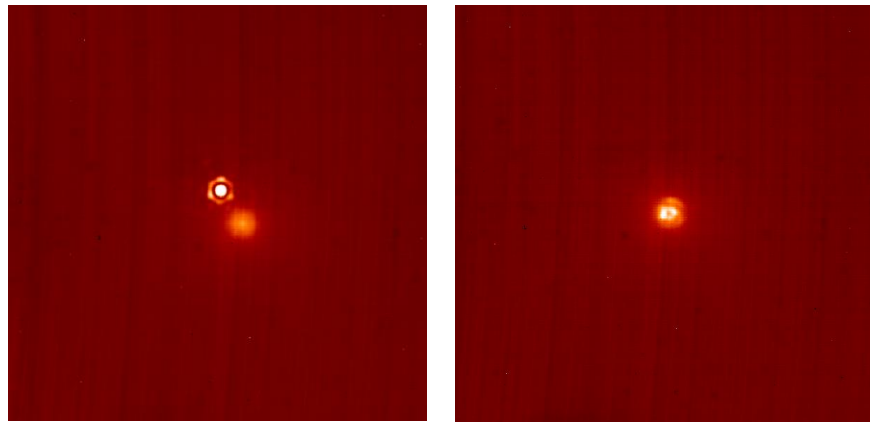


Figure 6: Left: L' image of HD 95650 offset to the upper-left of the vortex mask center. The vortex is the fuzzy glowing region at the FOV center. Right: L' image of HD 95650 roughly centered on the vortex. Attenuation on the PSF peak can clearly be seen.

The location of the target on the mask is optimized at the start of the sequence and subsequently updated at the end of each science exposure to point/track the PSF on the mask. A sample sequence of on-sky images in the L' filter demonstrating the convergence of the observing sequencer to track the target on the vortex mask is shown in Figure 7.

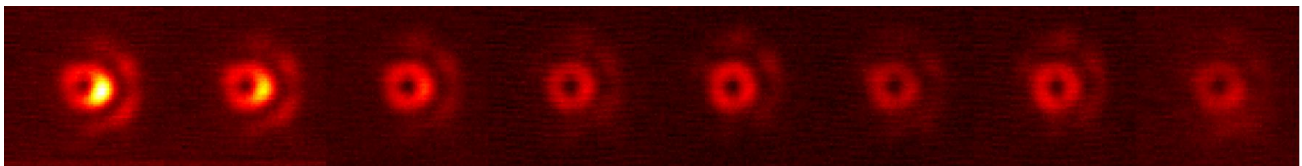


Figure 7: Convergence of the observing sequencer to track the target on the Vortex mask.

A sample QACITs science sequence consisting of 40 exposures in 512x512 pixels sub-window configuration using the Ms filter is shown in Figure 8. A sample science exposure using the coronagraph is shown on the left pane of Figure 8. The tip/tilt error estimated by the QACITs algorithm in closed-loop during the science sequence is shown in the middle pane. The colors indicate the age of the measurement, blue being the older data and red the newer values. The corresponding null depth is shown in the right pane.

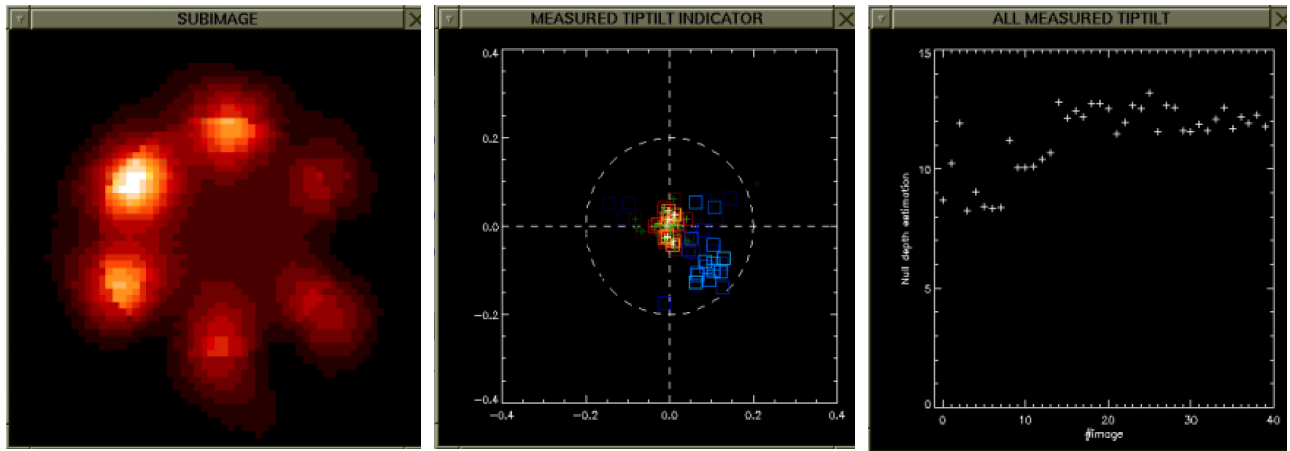


Figure 8: A sample on-sky QACITs sequence in the M-band. Left: The NIRC2 image in the Ms filter in the coronagraphic mode using the vortex mask optimized for the L- and M-bands. Middle: The tip/tilt error in arcseconds estimated by the QACITs in the closed-loop algorithm during a science sequence consists of 40 exposures. Right: The estimated null depth for the science sequence.

The performance improvement of the coronagraph, through the NIRC2 upgrade, is shown in Figure 9. Here typical single frames of a vortex science sequence, taken with the L', are shown, before and after the NIRC2 upgrade. In both cases, the PWS was used to drive the AO correction. The left image was taken with the old vortex mask and the *largehex* Lyot stop. The right image was taken with the new L-/M-optimized vortex mask and with the new *filxedhex* Lyot stop. The image taken with the old vortex mask and the *largehex* Lyot stop (left pane) still has remnants of the leftover PSF core. The combination of the new vortex mask and the Lyot stop clearly shows an improved suppression in the central area.

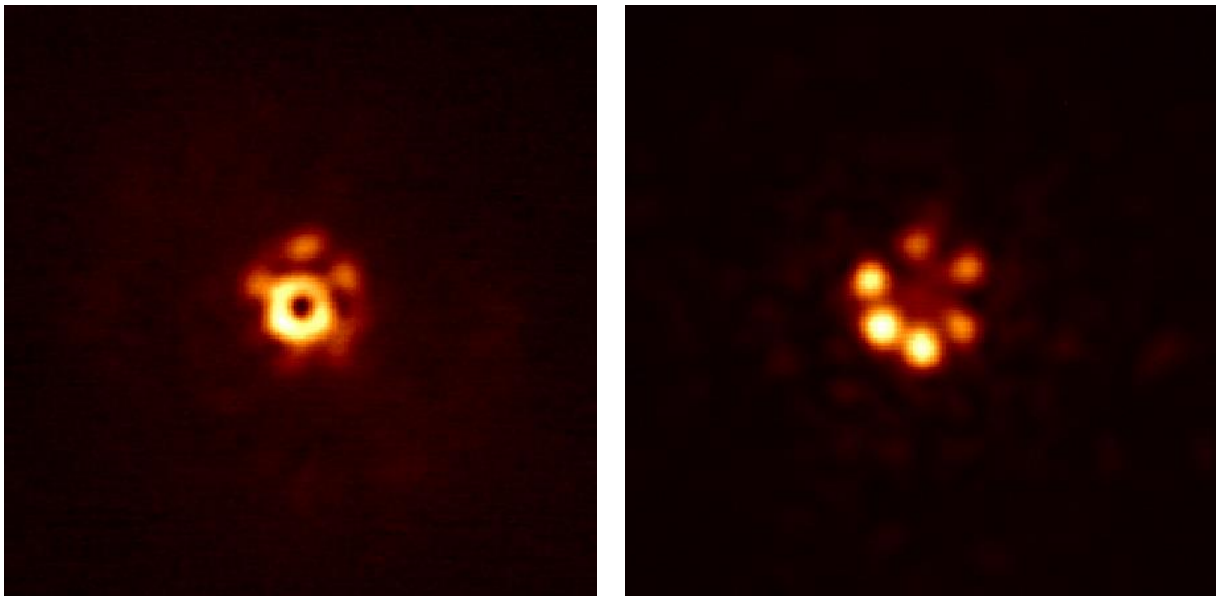


Figure 9: Comparison of coronagraphic images taken with the old (left) and the new (right) coronagraphic masks in the L' using the PWS. The target and the integration time are different for the two observations but represent typical individual science frames.

A comparison of the performance of the coronagraph that not only includes the impact of the new vortex but improvements in the calibration and use of the PWS compared to the Shack-Hartmann (SH-WFS) is shown in Figure 10. The measurements were taken on the same target (Eps Eri) using the Ms filter.

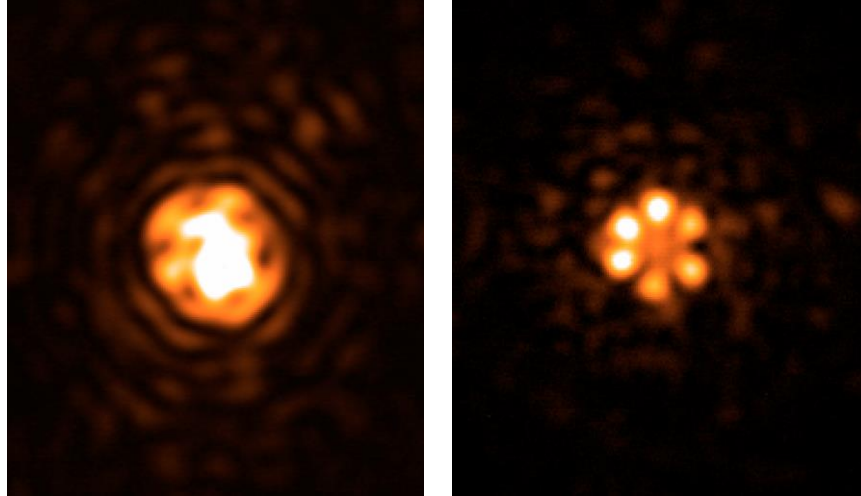


Figure 10: Comparison of coronagraphic images taken with the old mask using the SH-WFS (left) and the new mask using the PWS (right.)

6. SUMMARY AND FUTURE PLANS

We have presented details of the 2019 NIRC2 upgrade to enhance the performance of the near-infrared imager for coronagraphic observations. We have also shown some on-sky preliminary results. Even though the upgrade is already enabling unparallel high-contrast imaging science, we are already planning for a second phase of the upgrade to boost even more the NIRC2 science capabilities.

The plan for the second phase of the NIRC2 upgrade is:

1. To install a half-wave plate in the pupil simulator and to fully test the polarimetry mode.
2. To install an Amici prism (made out of ZnSe, BaF2, and Sapphire) that would enable spectro-polarimetry with $R > 100$ covering the full Y band to M band range.
3. To update the vortex observing sequencer (QACITs) for PWS field steering mirror control to enable large relative pointing offsets while the PWS loops are closed.
4. To implement a new operational tool for speckle nulling to enhance image contrast.
5. To upgrade the NIRC2 electronics in order to minimize the overhead in writing the data to disk and to enable short exposures using large/full frames.

ACKNOWLEDGMENTS

The data presented herein were obtained at the W. M. Keck Observatory, which is operated as a scientific partnership among the California Institute of Technology, the University of California, and the National Aeronautics and Space Administration. The Observatory was made possible by the generous financial support of the W. M. Keck Foundation.

The authors wish to recognize and acknowledge the very significant cultural role and reverence that the summit of Mauna kea has always had within the indigenous Hawaiian community. We are most fortunate to have the opportunity to conduct observations from this mountain.

REFERENCES

- Serabyn, E., Huby, E., Matthews, K., Mawet, D., Absil, O., Femenia, B., Wizinowich, P., et al., 2017, AJ, 153, 43
- Mawet, D., Choquet, E., Absil, O., Huby, E., Bottom, M., Serabyn, E., Femenia, B., et al., 2017, AJ, 153, 44
- Huby, E., Absil O., Mawet D., Baudoz, P., Femenia, B., Bottom, M., et al., 2016, SPIE, 9909, 20
- Huby, E., Bottom, M., Femenia, B., Ngo, H., Mawet, D., Serabyn, E., & Absil, O. , 2017, A&AAJ, 600, A46
- Ruane, G., Mawet, D., Kastner, J., Meshkat, T., Bottom, M., Femenia Castella, B., Absil, O., et. al., 2017, AJ, 154, 73
- Reggiani, M., Christiaens, V., Absil, O., Mawet, D., Huby, E., Choquet, E., Gomez Gonzalez, C., 2018, A&A, 611, A74